Impact of Stator Slot Shape on Cogging Torque of BLDC Motor

Karthick Kanagarathinam[1]* (iD)**, R. Manikandan[2]** (iD) **and Ravivarman S[3]** (iD)

[1]Associate Professor, Department of Electrical and Electronics Engineering, GMR Institute of Technology, Rajam, Andhra Pradesh, India. Email: kkarthiks@gmail.com, karthick.k@gmrit.edu.in
[2]Professor, Department of Electronics & Communication Engineering, Panimalar Engineering College, Chennai, Tamil Nadu, India. Email: money_kandan2004@yahoo.co.in
[3]Professor, Department of Electrical and Electronics Engineering, Vardhaman College of Engineering, Shamshabad, Hyderabad, Telangana, India. Email: ravivarman@vardhaman.org

***Correspondence:** kkarthiks@gmail.com, karthick.k@gmrit.edu.in

▨ **ABSTRACT-** Brushless DC (BLDC) motors have a wide range of applications in these modern days, such as electric vehicles, industrial robots, washing machines, pumps, and blowers. The brushless DC motors have many advantages when compared to induction motors and conventional DC motors, such as better speed control, noiseless operation, high efficiency, less maintenance, and a long life. Along with these benefits, there is one major disadvantage known as cogging, which causes undesirable effects in the motor such as noises and vibrations. BLDC motors have been widely used in automation and industrial applications due to their attractive features. There are certain parameters to be considered while designing a BLDC motor, such as its dimensions, number of windings turns, type of magnetic materials used, required torque, output current, slot-to-depth ratio, efficiency, temperature rise, etc. It is planned to minimize the cogging torque of BLDC motors by modifying the physical structure of the motors using mechanical methods, and the results will be evaluated using finite element analysis software. The results show that stator slot shapes (round, square, and airgap wedge) have cogging torques of 5.20 Nm, 0.4 Nm, and -0.296 Nm, respectively.

General Terms: Electrical Motors, Special Electrical Machines, Synchronous Speed Motors.
Keywords: BLDC, Cogging torque, FEA, Automation and Skewing.

1. INTRODUCTION

Brushless dc motors are famous in a broad variety of industrial applications, such as computer peripherals, servo-controlled structures, and electrical equipment, due to their robustness, simplicity, giant torque-to-volume ratio, and high efficiency. One of the best strategies is rotor/stator skewing. Skew, which is a well-established approach in literature, has some drawbacks like back-EMF distortion in BLDC motors where a trapezoidal form is desired. Another disadvantage of this method is the difficulty in manufacturing, particularly in large machines with conductor bars. The goal of this paper is to present the current evaluation of techniques for cogging torque discount by means of the capacity analysis of the finite element method [1]. The structure of the BLDC motor is shown in *figure 1*. The purpose of this study is to investigate the effect of stator slot shapes, such as round, square, and airgap wedge types, on cogging torque

magnitude. It is planned that the slot opening angle, slot depth, radial depth, and net output power be kept constant.
The merits of BLDC are

✓ The lack of brushes eliminates the need for frequent brush replacement, lowering maintenance costs.
✓ Because there are no brushes, sparking is reduced, and there are fewer chances of burnout due to sparking concerns.
✓ Brushless DC motors have a high ratio of torque to speed, which makes them perfect for robotics and medical uses.
✓ Because the brushless DC motor has no magnets, the heating issue is reduced.
✓ These motors can operate in either a low or no-load mode.
✓ Because there are no brushes, the working noise is reduced.
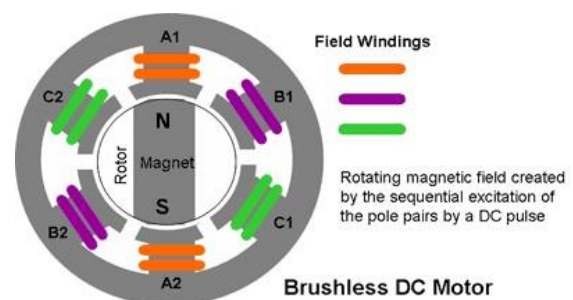✓ These motors are employed in electrical applications that need minimal noise.

Figure 1: PMBLDC motor

1.1 Principle of Operation of BLDC Motor

Figure 2 represents a permanent magnet brushless DC motor. Since the motor is brushless, its operation is explained with respect to the direction of the rotation of the permanent magnets and stator coil.

Each magnet has a direct axis (*d*-axis) coinciding with its centre line, *i.e.*, the main field flux and stator field flux are in quadrature with each other [2]. It works on the same principle as a DC motor, but it requires unidirectional torque in order to produce continuous rotation. The d-axis is the reference axis of the rotor, which helps to determine the position of the rotor. Assume that the coil is open-circuit; its flux linkage is the product of flux and number of turns and is a negative maximum when its axis is aligned with a magnet d-axis and the coil is facing the south pole.
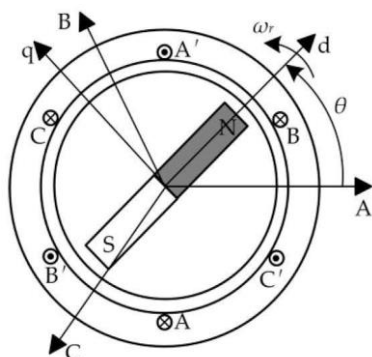

Figure 2: Permanent magnet under the influence of magnetic field

Figure 2 shows the position of the rotor 90° later. The coil axis is aligned with a *q*-axis or interpolar axis of the rotor, and the coil flux linkage is zero. Maximum flux linkage is reached after another 90° rotation at =180° [3].

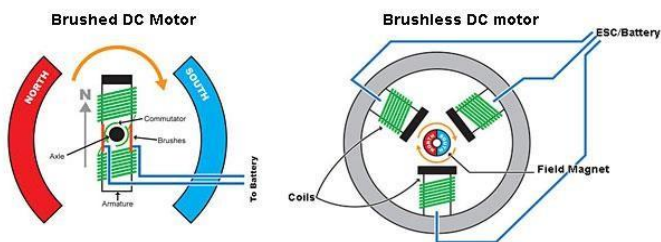## 1.2 Mechanical Commutation Vs Electronic Commutation

Figure 3: Brushed Vs Brushless DC Motor

In mechanical commutation, the function of the commutator and brush arrangement is to set up an armature mmf whose axis is always in quadrature with the main field mmf, irrespective of the speed of rotation of the motor, as shown in *figure 3*. While coming to electronic commutation, there will be a setup of the electronic commutation circuit, which is connected to the armature of the PMBLDC by means of a "rotor positioning sensor" (RPS) [4].
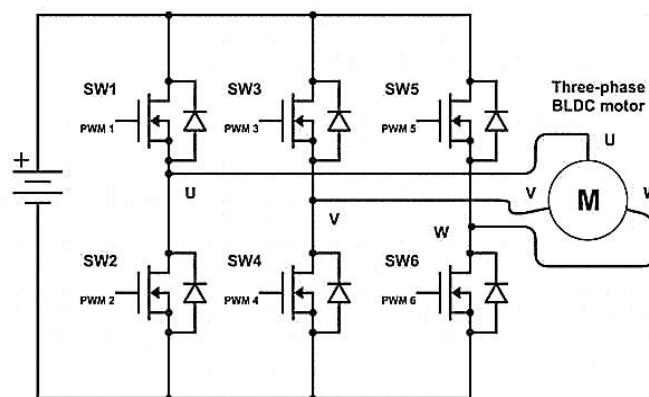

Figure 4: Electronic Commutation

Brushless motors use semiconductor switches to turn stator windings on and off when needed. Electronic commutation is a phrase derived from the term "commutator," which refers to the mechanism in dc motors that shifts current from one winding to the next, causing the rotor to turn as shown in figure 4.A four-pole permanent magnet and a smaller "sensing" magnet are included in the rotor of a conventional brushless motor [5]. The stator, on the other hand, is made up of three Hall-effect sensors and a three-phase, Y-connected winding. The sensor magnet indicates the position of the shaft by turning the Hall effect sensors "on" and "off." The controller can then transfer current to each winding at the optimal timing point using this information. These sensors help find the position of the rotor so as to give it excitation in order to produce unidirectional torque. These are some commonly used rotor positioning sensors.

- ✓ Automotive Rotor Position Sensors
- ✓ Resolver Position Sensor
- ✓ Inductive Position Sensor
- ✓ Hall Effect Position Sensor
- ✓ Magneto resistive Position Sensor

1.3 Role of BLDC Motor in Electric Vehicles

In the 21st century, electric vehicles became very prominent due to their attractive features and increased concern over pollution control in view of future possibilities. Compared to internal combustion engine vehicles, electric motor vehicles have their own advantages. The core parts of an electric vehicle are the motor and battery arrangement [6]. There are several types of motors employed in EVs, such as DC series, brushless DC, permanent magnet synchronous, three-phase AC induction motors, and switched reluctance motors. Among all of these BLDCs, are the most preferable due to their high efficiency of 95% to 98%. In this arrangement, commutation is performed electronically. BLDC motors are ideal for applications requiring a high-power density.

1.4 Finite Element Method (FEM)

There are numerous methods which can help us to analyze the cogging torque of PMBLDC motors, such as

- ✓ Virtual work method

✓ Maxwell stress tensor method

✓ Finite element method

✓ Coulomb virtual work method

✓ Nodal force method

For any design of the motor, a dependable physical model is crucial for analytical calculations, or "FEA."

 The Advantages of FEM are
✓ No prototype is required.
✓ Desirable parameters can be adjusted.
✓ FEM, as shown in Figure 5, is a reliable method to analyse the speed–torque characteristics of a PMBLDC motor.
✓ Cogging torque can be calculated numerically by either shifting the angle of the rotor or changing the direction of excitation of the stator.
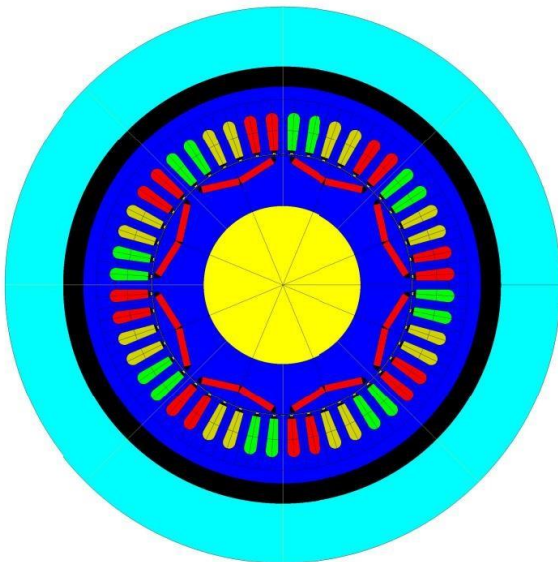

Figure 5: Finite Element Model

1.5 Related Works
Song, Y. et al. [13] investigated the impact of pole shoes and stator tooth structure variations on cogging torque. The proposed combination of novel tooth and novel pole shoe design is optimal for cogging torque with tangential magnetization.

Using the Virtual Work Method, Anuja TA et al. [14] developed an analytical expression for determining the shifting angle with the least cogging torque in the PMBLDC motor. 3D FEA was used to study the optimization of the shifting angle with the least amount of cogging torque. A rotor with an asymmetrical magnet construction is recommended in this method for minimizing cogging torque. The asymmetry is created by displacing the PM. The shifting angle used in the analysis was chosen by keeping the L/τ ratio within the allowable range. After defining the dynamic model of the BLDC motor, K. Prathibanandhi et al. [15] produced a control approach, and the Matlab/Simulink model is used to create the electronic interface with the BLDC

motor, while tactically using Xilinx tools for various types of co-simulation over the same model.

A slotless BLDC motor with toroidal winding was developed by Lee H-Y et al. [16]. Toroidal winding is accomplished by wrapping a coil around a ring-type stator yoke. FEA findings were compared to the prototype's resistance, back EMF, cogging torque, and performance. The air gap flux density and winding factor had a 2% inaccuracy, whereas the back EMF had a 10% error. The recommended slotless motor shows a basic way to make BLDC slotless motors with toroidal windings that don't have slots.

Ho, S.L. et al. [17] describe using FEM to calculate the cogging torque profile of PM motors when the distribution of PM is unequal. The suggested approach drastically reduces the computation time to solve the cogging torque issue to 0.06 % of that required by regular FEM. Cogging torque is affected by a number of BLDC motor design factors, including air gap length, slot opening, and magnet pole pitch. These methods include altering slot and tooth widths, employing PM skewing, generating auxiliary teeth, using slot-less armatures, and adding notches in the rotor structure. A slot-less core has a lower inductance and may thus operate at higher speeds. The lack of teeth in the lamination stack reduces cogging torque, making it appropriate for low-speed operations as well [18-20]. The main disadvantage of a core without slots is that it is more expensive since it requires more winding to fill the larger air gap. In this research, we analyzed the suitable slot shape that has a major impact on cogging torque. The following section describes the design and mathematical analysis of the BLDC motor.

2. DESIGN AND MATHEMATICAL ANALYSIS
2.1 General Sizing of Stator
We adopted the design of PMBLDC motor from [21-23]. Initially, the total flux has to be fixed. It is beneficial to identify how the dimensions of the ferro magnetic portions of the rotor are related to the number of magnet poles, the number of slots, and the rotor outside radius. The total flux across the airgap can be represented as in *equation (1)* if the alternating direction of flux flow is ignored.

$$\Phi_{Total} = B_g A_g = 2\pi B_g R_{ro} L_{st} \qquad (1)$$

$$\Phi_t = \frac{\Phi_{total}}{N_s} = \frac{B_g 2\pi R_{ro} L_{st}}{N_s} \qquad (2)$$

This tooth flux flows through the tooth body, resulting in a flux density of magnitude as

$$B_t = \frac{\Phi_t}{w_{tb} K_{st} L_{st}} \qquad (3)$$

During the motor design process, the tooth width w_{tb} is adjusted to keep the flux density of both ferromagnetic materials below the saturation value. Once B_t is set, substitution of *equation (2)* into *equation (3)* simple algebra gives the tooth body width as

$$W_{tb} = \frac{2\pi R_{ro} B_g}{N_s K_{st} B_t} \qquad (4)$$

According to the preceding expression, the tooth body width is directly proportional to the rotor outer radius. Therefore, as R_{ro} increases, w_{tb} increases at the same relative pace. In addition, w_{tb} is inversely proportional to the number of stator slots N_s. The tooth body width reduces proportionally as the number of slots rises [8]. The number of magnet poles N_m does not appear in *equation (1)*. Because the overall flux traversing the air gap is independent of the number of magnet poles. Therefore, w_{tb} does not influence as N_m varies. When each magnet's flux divides into two parts, each half forming a flux loop with one half of the flux from the adjacent magnet, As such, one half of the flux from each magnet travels through the stator and rotor yokes. At the rotor and stator yokes' radial lines, this flux creates flux densities in the stator yoke and rotor yoke as given in *equation (5) & (6)* respectively.

$$B_{sy} = \frac{\Phi_{total}/2}{w_{sy}K_{st}L_{st}} \qquad (5)$$

$$B_{ry} = \frac{\Phi_{total}/2}{w_{ry}K_{st}L_{st}} \qquad (6)$$

Where Φ_{total} in this case is the total flux leaving one magnet. Substitution of *equation (1)* into *equation (5) and (6)* leads to expressions for the stator and rotor yoke widths of

$$W_{sy} = \frac{\pi R_0 B_g}{N_m K_{st} B_{sy}} \qquad (7)$$

And $$W_{ry} = \frac{\pi R_0 B_g}{N_m K_{st} B_{ry}} \qquad (8)$$

respectively.

2.2 Cogging Torque
Cogging torque in a PMBLDC motor is an objectionable phenomenon and occurs due to the interactions of rotor and stator PMs. It is represented as in *equation (9)*.

$$T_{cog} = \frac{1}{2} \Phi_g^2 \frac{dR}{d\theta} \qquad (9)$$

Where Φ_g - Airgap flux

    R - Airgap reluctance

    θ - Rotor position

▦ 3. RESULTS AND DISCUSSION
A model for creating geometry and mesh with overlay is shown in *figure 6*. Steps to be followed to create geometry and meshes:

✓ Open the Altair Flux software and select a new 2D project.
✓ Now, click on extensions, and then click on overlay.
✓ Select and load a certified overlay. Brushless Permanent Magnet Motors V11.1. PFOA can be loaded by selecting the overlay. After loading the model, select "New Motor BPM," then "General," and finally "Infinite" [9].
✓ Now input the values of the inner and outer radii.
✓ Click on the air gap and assign some value.

✓ Click on the rotor and assign all the required parameter values, such as magnet shape, shaft radius, thickness of magnet, magnet pole arc, and number of magnet blocks per pole.
✓ After that, click on rotor embedded magnet type, magnet shape, number of poles, rotor external radius, and rotor shift angle [10–12].
✓ Now click on the stator and select slot shape, slot opening, radial depth, slot depth, tooth width on the stator, and slot opening angle.
✓ After that, click on "general" and select the number of slots, lamination shape, and stator outer radius.
✓ Click on "winding" and select "classical winding," "type of winding," "number of phases," and "number of coils per pole per phase."
✓ Edit mesh points for the air gap and rotor.
✓ Select physical parameters such as magnet material, type of mechanic set, type of load, visibility, and color.
✓ Now choose the limits of the rotor's angular position and figure out the cogging torque.
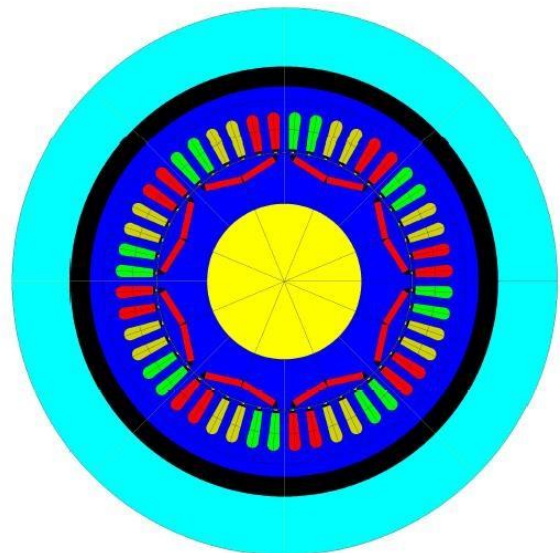✓ The same steps are followed for every individual case of cogging torque.

Figure 6: Finite Element Model of case 1

3.1 Stator round
✓ A brushless permanent magnet motor V11.1.PFO overlay has been chosen.
✓ The rotor parameters are 110mm inner radius, 140mm outer radius, 0.6mm airgap, and rotor lpm magnet shape (creating geometry and mesh).
✓ The chosen stator parameters are: stator round slot shape; slot opening of 2mm; radial depth of 1mm; slot depth of 30mm; tooth width of 6.5mm; and slot opening degree of 40 degrees (creating geometry and mesh).
✓ After that, the lap winding is selected, and different mesh points for the airgap, rotor magnet, magnet material, and

mechanical sets for the rotor and stator are edited (defining the physics).

✓ Finally, after creating geometry and meshes and defining the physics, the particular scenario is solved (defining the solving scenario).
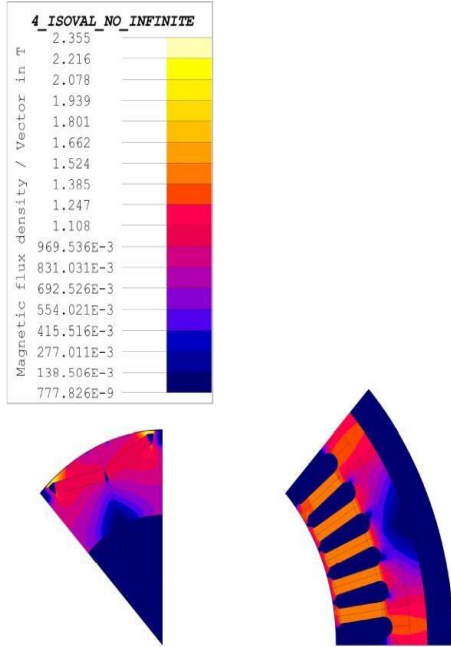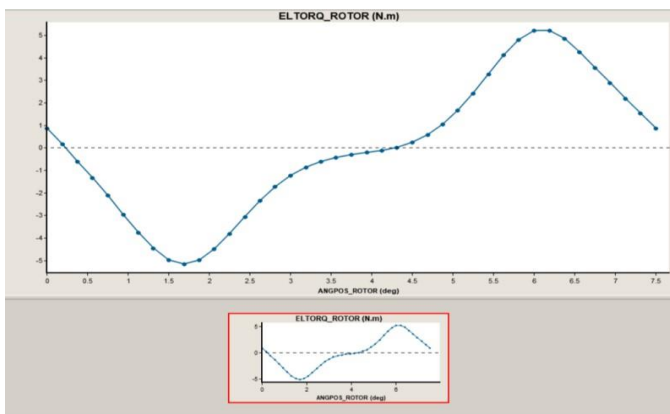

Figure 7: Flux distribution of case 1

Figure 8: Angular Position of the rotor and cogging torque of BLDC Motor for Case 1

3.2 Stator Square

✓ A brushless permanent magnet motor V11.1.PFO overlay has been chosen.

✓ The rotor parameters are 110mm inner radius, 140mm outer radius, 0.6mm airgap, and rotor lpm magnet shape (creating geometry and mesh).

✓ The stator parameters chosen are as follows: stator round slot shape; slot opening of 2mm; radial depth of 1mm; slot depth of 30mm; stator tooth width of 6mm; and slot opening degree of 40 degrees (creating geometry and mesh).

✓ After that, the lap winding is selected, and different mesh points for the airgap, rotor magnet, magnet material, and mechanical sets for the rotor and stator are edited (defining the physics).

Figure 9 shows the finite element model for *Case 2*. *Figure 10* shows the flux distribution in case 2. *Figure 11* shows the angular position and resultant cogging torque of *Case 2*.
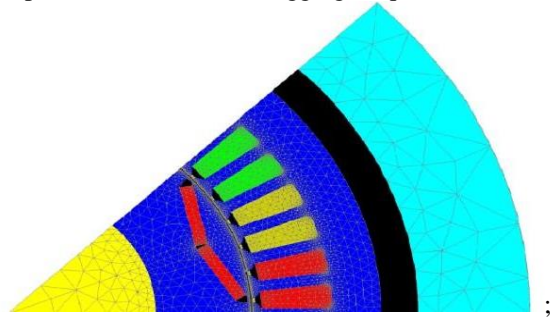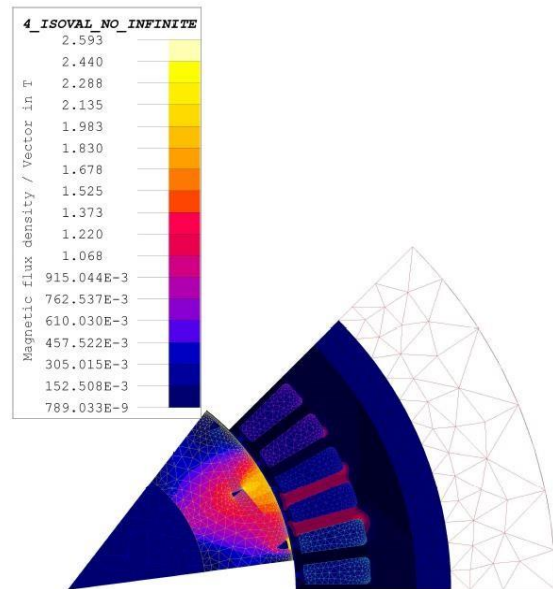

Figure 9: Finite Element Model of case 2
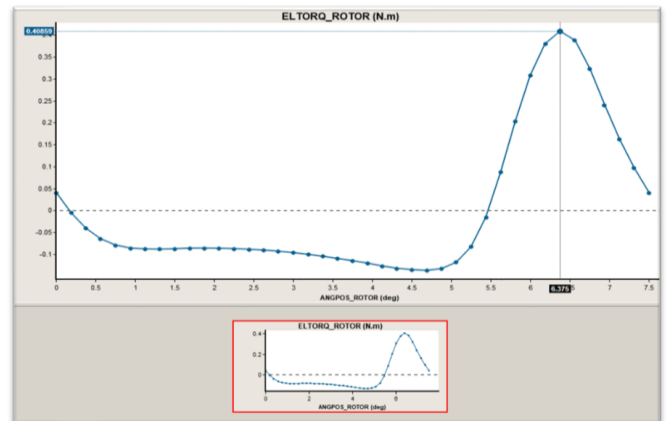

Figure 10: Flux distribution of case 2

Figure. 11: Angular Position of The Rotor and Cogging Torque of BLDC Motor for Case 2

International Journal of
Electrical and Electronics Research (IJEER)
Research Article | Volume 11, Issue 1 | Pages 54-60 | e-ISSN: 2347-470X

FOREX Publication
Open Access | Rapid and quality publishing

3.3 Stator Airgap Wedge

- ✓ A brushless permanent magnet motor V11.1.PFO overlay has been chosen.
- ✓ The rotor parameters are 110mm inner radius, 140mm outer radius, 0.6mm airgap, and rotor lpm magnet shape (creating geometry and mesh).
- ✓ The chosen stator parameters are: stator round slot shape; slot opening of 2mm; radial depth of 1mm; slot depth of 30mm; tooth width of 5.5mm; and slot opening degree of 40 degrees (creating geometry and mesh).
- ✓ After that, the lap winding is selected, and different mesh points for the airgap, rotor magnet, magnet material, and mechanical sets for the rotor and stator are edited (defining the physics).
- ✓ Finally, after creating geometry and meshes and defining the physics, the particular scenario is solved (defining the solving scenario).

Figure 10 shows the finite element model for *Case 3*. *Figure 11* shows the flux distribution in *Case 3*. *Figure 12* shows the angular position and resultant cogging torque of *Case 3*.

Table 1: Comparison Table for the three Cases

Stator slot shape	Stator round	Stator square	Stator airgap wedge
Slot opening	2	2	2
Radial depth	1	1	1
Slot depth	30	30	30
Tooth width stator	6.5	6	5.5
Slot opening angle	40	40	40
Cogging torque (Nm)	5.20	0.400	-0.296

The tooth fillet radius is taken as zero due to its low value of approximately 0.25 to 0.3 based on the design parameter for standardization.
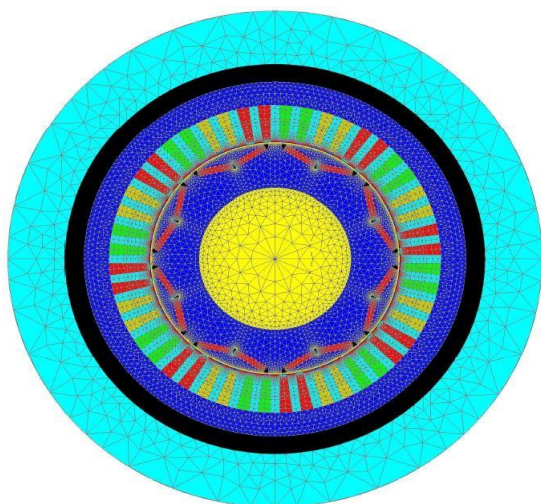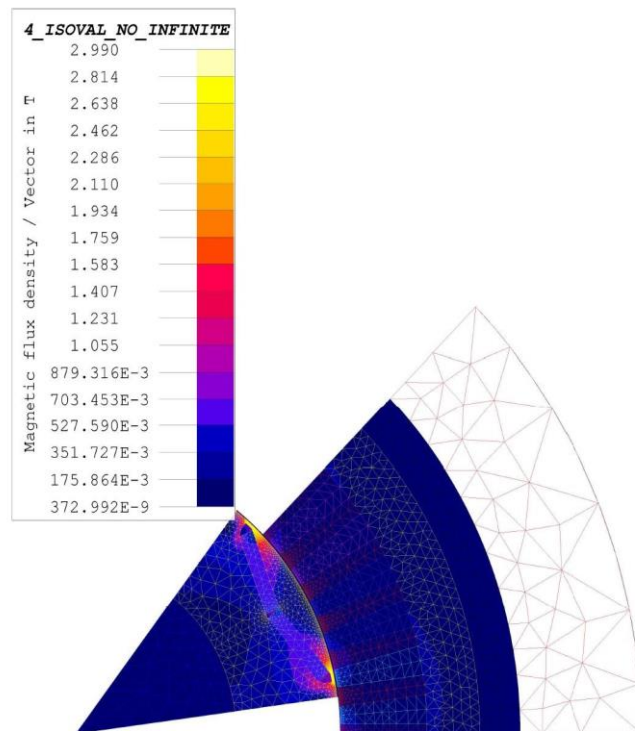

Figure 12: Finite Element Model of case 3

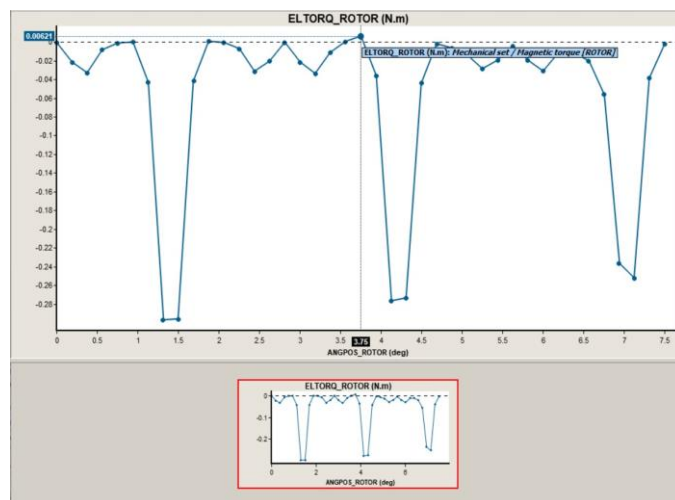**Figure 13:** Flux distribution of Case 3

Figure 14: Angular Position of the Rotor and Cogging Torque of BLDC Motor for Case 3

4. CONCLUSION

After performing finite element analysis on a model, a reduction in cogging torque has been achieved. In this paper, a software called "ALTAIR FLUX" has been introduced for the design and analysis purposes of the BLDC motor. In that software, a MOTOR PRIUS 2 BLDC model has been taken, and all the required parameters are given. The experiment was conducted under the assumptions of constant speed and constant load. In addition, magnetic materials (magnet and NdFeB) from the Altair database were used. To reduce the cogging torque, the

stator slot shape has been modified into four different types. The results clearly show that changing the shape of the stator slots had a significant impact on the cogging torque. The results show that cogging torque maximum peak values are 7.81 Nm, 5.20 Nm, and 0.400 Nm for stator GH, depending on the round or square shape of the stator slots. Compared to the stator GH slot shape, the stator round shape has a reduced cogging torque value of 33.4%. The maximum cogging torque reduction obtained with stator square-shaped slots is 94.8%. There are some papers where the authors propose different approaches (both mechanical and electrical methods) to achieve cogging torque reduction, but this paper proposes a mechanical approach in the design of the BLDC motor.

This paper mainly focused on how cogging torque has been changing with respect to the shape of the stator slot. The maximum speed is set to 6000 rpm, and the slot depth has been chosen as 30 mm, such that it has an impact on the diameter of the core (*i.e.*, the outer diameter, which is 242 mm).

⁂ REFERENCES

[1] I. -H. Jo, H. -W. Lee, G. Jeong, W. -Y. Ji and C. -B. Park, "A Study on the Reduction of Cogging Torque for the Skew of a Magnetic Geared Synchronous Motor," in IEEE Transactions on Magnetics, vol. 55, no. 2, pp. 1-5, Feb. 2019, Art no. 8100505, doi: 10.1109/TMAG.2018.2873310.

[2] Karthick, K., Premkumar, M., Manikandan, R. and Cristin, R. 2018. Survey of Image Processing Based Applications in AMR. Review of Computer Engineering Research. 5, 1 (Sep. 2018), 12–19. DOI: https://doi.org/10.18488/journal.76.2018.51.12.19.

[3] Loheswaran, K, Daniya, T, Karthick, K, Hybrid Cuckoo Search Algorithm with Iterative Local Search for Optimized Task Scheduling on Cloud Computing Environment. Journal of Computational and Theoretical Nanoscience, Volume 16, Numbers 5-6, May 2019, pp. 2065-2071(7), American Scientific Publishers, DOI: https://doi.org/10.1166/jctn.2019.7851

[4] C. He and T. Wu, "Permanent magnet brushless DC motor and mechanical structure design for the electric impact wrench system," Energies, vol. 11, no. 6, p. 1360, 2018.

[5] K. Karthick, S. Ravivarman, Ravi Samikannu, K. Vinoth, Bashyam Sasikumar, "Analysis of the Impact of Magnetic Materials on Cogging Torque in Brushless DC Motor", Advances in Materials Science and Engineering, vol. 2021, Article ID 5954967, 10 pages, 2021. https://doi.org/10.1155/2021/5954967

[6] T. Srisiriwanna and M. Konghirun, "A study of cogging torque reduction methods in brushless dc motor," 2012 9th International Conference on Electrical Engineering/Electronics, Computer, Telecommunications and Information Technology, 2012, pp. 1-4, doi: 10.1109/ECTICon.2012.6254191.

[7] K. Karthick & S. Chitra (2017) Novel Method for Energy Consumption Billing Using Optical Character Recognition, Energy Engineering, 114:3, 64-76, DOI: 10.1080/01998595.2017.11863765

[8] M. R. Hazari, E. Jahan, M. E. Siraj, M. T. I. Khan and A. M. Saleque, "Design of a Brushless DC (BLDC) motor controller," 2014 International Conference on Electrical Engineering and Information & Communication Technology, 2014, pp. 1-6, doi: 10.1109/ICEEICT.2014.6919048.

[9] K. B. Ravindrakumar, K. Karthick, D. Sivanandakumar, S. Sivarajan, "Fuzzy Based Approach for Direct Torque Control of Three Phase Induction Motor", International Journal of Scientific & Technology Research, Volume 8, Issue 10, October 2019 ISSN 2277-8616.

[10] H. Nory and Y. Akyün, "Experimentally Constrained Design Parameters Approach for PMSM and BLDC Motor," 2020 6th International Conference on Electric Power and Energy Conversion Systems (EPECS), 2020, pp. 123-129, doi: 10.1109/EPECS48981.2020.9304526.

[11] Karthick, K., Jaiganesh, K., Kavaskar, S. (2021). Comprehensive Study, Design and Economic Feasibility Analysis of Solar PV Powered Water Pumping System. Energy Engineering, 118(6), 1887–1904. doi:10.32604/EE.2021.017563

[12] Jun-Uk Chu, In-Hyuk Moon, Gi-Won Choi, Jei-Cheong Ryu and Mu-Seong Mun, "Design of BLDC motor controller for electric power wheelchair," Proceedings of the IEEE International Conference on Mechatronics, 2004. ICM '04., 2004, pp. 92-7e, doi: 10.1109/ICMECH.2004.1364418.

[13] Song, Y., Zhang, Z., Yu, S., Zhang, F. and Zhang, Y. (2021), Analysis and reduction of cogging torque in direct-drive external-rotor permanent magnet synchronous motor for belt conveyor application. IET Electr. Power Appl, 15: 668-680. https://doi.org/10.1049/elp2.12048

[14] Anuja TA, Doss MAN. Reduction of Cogging Torque in Surface Mounted Permanent Magnet Brushless DC Motor by Adapting Rotor Magnetic Displacement. Energies. 2021; 14(10):2861. https://doi.org/10.3390/en14102861

[15] K. Prathibanandhi, C. Yaashuwanth, Adam Raja Basha, Improved torque performance in BLDC-motor-drive through Jaya optimization implemented on Xilinx platform, Microprocessors and Microsystems, Volume 81, 2021, 103681, ISSN 0141-9331, https://doi.org/10.1016/j.micpro.2020.103681.

[16] Lee H-Y, Yoon S-Y, Kwon S-O, Shin J-Y, Park S-H, Lim M-S. A Study on a Slotless Brushless DC Motor with Toroidal Winding. Processes. 2021; 9(11):1881. https://doi.org/10.3390/pr9111881

[17] Ho, S.L., Chen, N., & Fu, W.N. (2010). An Optimal Design Method for the Minimization of Cogging Torques of a Permanent Magnet Motor Using FEM and Genetic Algorithm. IEEE Transactions on Applied Superconductivity, 20, 861-864.

[18] Abhishek Arora and Janardan Kesari (2022), Design and Development of a Solar Electric Delivery Pod. IJEER 10(3), 429-437. DOI: 10.37391/IJEER.100304.

[19] Jayesh Tripathi, Krishna Sharma and J.N. Rai (2022), Speed Control Analysis of Brushless DC Motor Using PI, PID and Fuzzy-PI Controllers. IJEER 10(3), 470-474. DOI: 10.37391/IJEER.100311.

[20] Gaurav Gadge and Yogesh Pahariya (2022), Grey Wolf Optimization Based Energy Management Strategy for Hybrid Electrical Vehicles. IJEER 10(3), 772-778. DOI: 10.37391/IJEER.100359.